



Published in final edited form as:

*Mol Carcinog.* 2019 November ; 58(11): 2017–2025. doi:10.1002/mc.23093.

## Serum miR-182 is a predictive biomarker for dichotomization of risk of hepatocellular carcinoma in rats

Merricka C. Livingstone<sup>a</sup>, Natalie M. Johnson<sup>b</sup>, Bill D. Roebuck<sup>c</sup>, Thomas W. Kensler<sup>a,d</sup>, John D. Groopman<sup>a</sup>

<sup>(a)</sup>Department of Environmental Health and Engineering, Johns Hopkins Bloomberg School of Public Health, Baltimore, MD 21205;

<sup>(b)</sup>Department of Environmental and Occupational Health, Texas A&M School of Public Health, College Station, TX 77843;

<sup>(c)</sup>Department of Pharmacology and Toxicology, Giesel School of Medicine at Dartmouth, Hanover, NH 03755;

<sup>(d)</sup>Department of Pharmacology and Chemical Biology, University of Pittsburgh School of Medicine, Pittsburgh, PA 15261

### Abstract

Exploration of animal models lead to discoveries that can reveal candidate biomarkers for translation to human populations. Herein, a model of hepatocarcinogenesis and protection was used in which rats treated with aflatoxin (AFB<sub>1</sub>) daily for 28 days (200 µg/kg BW) developed tumors compared with rats completely protected from tumors by concurrent administration of the chemoprotective agent, 1-[2-cyano-3-,12-dioxooleana-1,9(11)-dien-28-oyl]imidazole (CDDO-Im). Differential expression of miRNAs in tumors (AFB<sub>1</sub>) and non-tumor (AFB<sub>1</sub>+ CDDO-Im) bearing livers and their levels in sera over the life-course of the animals was determined. miRNA transcriptome analysis identified 17 miRNAs significantly upregulated at greater than five-fold in the tumors. The ten most dysregulated miRNAs judged by fold-change and biological significance were selected for further study, including liver specific miR-122-5p. Validation of sequencing results by real-time PCR confirmed the upregulation of the majority of these miRNAs in tumors, including miR-182, as well as miR-224-5p as the most dysregulated of these miRNAs (over 400-fold). Longitudinal analysis of levels of miR-182 in sera demonstrated significant and persistent increases (5.13 fold; 95% CI: 4.59–5.70). The increase in miR-182 was detected months before any clinical symptoms were present in the animals. By the terminal time point of the study, in addition to elevated levels of serum miR-182, serum miR-122-5p was also found to be increased (>1.5 fold) in animals that developed hepatocarcinomas. Thus, using data from an unbiased discovery approach of the tissue findings, serum miR-182 was found to track across the complex, multistage process of hepatocarcinogenesis opening an opportunity for translation to human populations.

**Corresponding Author:** Merricka C. Livingstone, 615 N. Wolfe St., Rm E7402, Baltimore, MD, USA 21205., Telephone: 321-258-8726; mliving8@jhu.edu.

**Data Availability Statement:**

Data on the miRNA analysis will be available on request to the corresponding author.

## Keywords

miRNA; aflatoxin B<sub>1</sub>; CDDO-Im; RNA sequencing; hepatocarcinogenesis

---

## 1. Introduction

Hepatocellular carcinoma (HCC) continues to be a major health problem worldwide, claiming nearly 830,000 lives in 2016<sup>1</sup>. Most HCC is conceptually preventable since the major risk factors have been characterized; however, mortality rates still remain high. This is partially due to the typical diagnosis of patients during the advanced stages of disease when symptoms are more apparent, but treatment is not often effective<sup>2</sup>. The 5-year overall survival rate for patients detected in early stages is over 50%, but that rate universally drops to less than 16% when diagnosis occurs at later stages<sup>3–5</sup>. It is crucial to have effective early surveillance to identify those who could benefit the most from therapeutic interventions. Current strategies include imaging and measuring serum  $\alpha$ -fetoprotein (AFP) and des-gamma carboxyprothrombin (DCP) levels. Imaging by ultrasound or computed tomography (CT) is a primary method for tumor detection but these instruments may not be readily accessible in economically poor countries where the rates of HCC are among the highest in the world<sup>6,7</sup>. Finally, the serum biomarkers currently used have poor sensitivity and specificity during early stage disease further complicating prevention strategies<sup>5</sup>.

MicroRNAs (miRNAs, miRs) are short non-coding RNAs that can modulate the expression of target messenger RNAs (mRNAs). They have been demonstrated to be dysregulated in experimental and human HCC and have emerged as promising disease biomarkers because of their stability and sequence homology between species, especially in mammals<sup>8–14</sup>. MicroRNAs can be detected in the circulation<sup>15,16</sup>. Studies have identified a variety of miRNAs that differentiate HCC patients from healthy controls<sup>17–25</sup>. Over expression of tissue miRs-34a, 200a, 221 and serum miR-224 have been associated with poor prognosis in HCC patients<sup>11,17,26–28</sup>. Limited experimental information has been revealed about miRNAs in aflatoxin-induced HCC but several investigations to date have focused on an acute exposure period and genotoxic effects of aflatoxin on miRNAs<sup>29,30</sup>.

Our previous study identified a panel of miRNAs that were dysregulated in hepatic tissue and sera at the end of a 4-week carcinogenic AFB<sub>1</sub> dosing regimen both with and without chemoprotection<sup>31</sup>. The miRNAs rno-miR-122-5p, 34a-5p, and 181c-3p were found to be increased in the livers and sera of animals dosed with AFB<sub>1</sub>. Animals co-exposed to the chemopreventive agent 1-[2-cyano-3-,12-dioxooleana-1,9(11)-dien-28-oyl]imidazole (CDDO-Im) were protected from the genotoxic insult of aflatoxin and displayed near-basal hepatic expression of candidate miRNAs. CDDO-Im is an analog of the drug bardoxolone-methyl currently in clinical trials, and is a potent activator of Nrf2 signaling that leads to enhanced aflatoxin detoxication<sup>32,33</sup>. For the current study, we sought to determine dysregulated miRNAs that longitudinally emerge in sera during the lifetime of the animals and in the sera of the rats with HCC at termination. Initial discovery experiments used RNA sequencing and real-time PCR in tumor tissue induced by aflatoxin and non-tumor hepatic tissue from both untreated and AFB<sub>1</sub> plus CDDO-Im co-exposed animals. The miRNA

profile was dramatically altered in tumors when compared to non-tumor bearing livers. These data identified a panel of miRNAs that were highly dysregulated due to aflatoxin treatment and led to the finding that in circulation, following the dosing protocol, miR-182 was consistently increased by more than 5-fold throughout the life-course of animals subsequently diagnosed with HCC.

## 2. Materials & Methods

### 2.1 Biological Sample Selection

Tumor samples were obtained from a lifetime bioassay that has been previously described<sup>34</sup>. Male F344 rats were randomly assigned to two treatment groups: 200 µg/kg body weight (BW) AFB<sub>1</sub> daily for four weeks, or 200 µg/kg BW AFB<sub>1</sub> daily for four weeks plus 30 µmol/kg BW rat CDDO-Im three times per week starting one week before AFB<sub>1</sub> dosing and continuing throughout the exposure period. All animals were maintained on a control diet following the dosing regimen<sup>34</sup>. Animals were followed during their lifetime for development of hepatocellular carcinoma. HCC diagnoses were histologically confirmed according to Eustis *et al.*<sup>35</sup>. All rats had multiple HCCs ranging from 13 to 20 per liver, and the time of sacrifice ranged between 79 and 95 weeks of age (Table S1). Photos of the livers that were screened for miRNAs at the termination of this study from the AFB<sub>1</sub> and AFB<sub>1</sub> plus CDDO-Im groups are found in Figure S1 and examples of typical histopathology of these HCCs arising in the AFB<sub>1</sub> group are shown in Figure S2. All experiments were approved by The Johns Hopkins University Animal Care and Use Committee.

Tumors from animals previously dosed with AFB<sub>1</sub> were selected for further analysis based on clear demarcation of a large single tumor as opposed to multiple coalesced tumors. Sections of non-tumor hepatic tissue from untreated animals and those dosed with AFB<sub>1</sub> plus CDDO-Im were also excised. There were no tumors in any of these animals. In addition, sera from corresponding animals were analyzed from various time points of the bioassay.

### 2.2 RNA Isolation

**2.2.1 Rat tumor & non-tumor tissue:** Total RNA was isolated from approximately 10 mg liver tissue or tumor using the miRCURY Isolation tissue kit (Exiqon, Vedbaek, Denmark) according to the manufacturer's protocol. RNA was eluted with 50µL elution buffer (provided by manufacturer).

**2.2.2 Rat sera:** Small RNAs (<1000 nts) were isolated from 50 µL serum using the miRCURY miRNA Isolation kit for biofluids (Exiqon, Vedbaek, Denmark) according to the manufacturer's protocol. RNA was eluted with 50 µL RNase-free water (provided by manufacturer).

### 2.3 Small RNA Sequencing

Total RNA from tumors and non-tumor tissue samples with an RNA Integrity Number (RIN) greater than 7 identified using the 2100 Bioanalyzer (Agilent, Santa Clara, CA) were selected for sequencing. Small RNA libraries were generated using the TruSeq Small RNA

Sample Preparation kit (Illumina, San Diego, CA) following the manufacturer's protocol. Samples were prepared with a unique index and sequenced across one lane with single-end 50 bp reads. The cDNA libraries were sequenced using the HiSeq 2000 platform (Illumina, San Diego, CA).

## 2.4 RNA sequencing analysis

Contaminant reads with lengths less than 15 bp and a phred score less than 20 were discarded from the total output reads. The processed reads were aligned to miRNA sequences in the rat genome by conducting a BLAST search (NCBI, v.2.2.30) against a built database of rat miRNA sequences downloaded from miRBase v. 21 ([www.mirbase.org](http://www.mirbase.org))<sup>36</sup>. Hits were counted that aligned perfectly to the seed sequence, and to at least 90% of the length of the miRNA with at least 90% identity. Normalization of the count data was calculated using *estimateSizeFactors*. The variance estimation was calculated using *estimateDispersions*. Count data was averaged across all biological replicates for each treatment group and normalized to reads per million miRNA reads for each miRNA across all treatment groups (Equation 1). DESeq (Bioconductor) was used for differential expression analysis.

$$\begin{aligned} & \text{number of reads per million miRNA reads} \\ &= \frac{\text{total miRNA count}}{\text{total read count for treatment group} \bullet 10^{-6}} \end{aligned} \quad (\text{Equation 1})$$

## 2.5 Candidate microRNA selection

Using the count data, a list was created containing the miRNAs that had greater than five-fold change between the AFB<sub>1</sub>-treated and control groups. From that list, a candidate list was generated that contained the top dysregulated miRNAs as well as functional information. A finalized panel of ten candidate miRNAs was determined that included the most dysregulated miRNAs with known biological significance from the literature.

## 2.6 MicroRNA expression analysis

Nine ng of eluted total RNA from tumor or tissue was reverse transcribed (RT) using miRNA specific stem-loop primers and the TaqMan miRNA Reverse Transcription Kit following the manufacturer's instructions (Applied Biosystems, Foster City, CA). Four  $\mu$ L of eluted small RNA from sera of corresponding animals was also processed in the same manner. The expression levels of candidate miRNAs were measured by real-time PCR (qPCR) using TaqMan miRNA assays (Applied Biosystems) and the StepOne Plus System (Applied Biosystems). All assays were analyzed in triplicate. The relative amount of each miRNA was calculated using the  $2^{-Ct}$  method<sup>37</sup>

## 2.7 Statistical Methods

Analysis of variance (ANOVA) followed by Tukey's multiple comparison test was used to analyze validation PCR experiments. Statistical analyses were performed using GraphPad Prism 7.0 software. Graphs indicate mean  $\pm$  SD unless noted otherwise. A generalized estimating equations (GEE) model with an exchangeable correlation structure was used to

analyze the longitudinal data to determine fold change with Stata 15 statistical software package. Level of significance was set at  $P < 0.05$  (\* $P < 0.05$ , \*\* $P < 0.005$ , \*\*\* $P < 0.001$ ).

### 2.7.1 Example Stata command for GEE analysis

```
use "D:\GEE analysis\mmm_182full.dta", clear
xtset animal weeksofage
destring tx, gen(txn)
drop tx
rename txn tx
xtgee mir182ct tx, family(gaussian) corr(exc) eform robust
```

## 3. Results

### 3.1 Unique global miRNA profile in aflatoxin-induced tumors

Total RNA isolated from five hepatic tumors, each from different animals (Figure S1) initiated with AFB<sub>1</sub>, were sequenced. Liver tissues were also sequenced from five animals dosed with AFB<sub>1</sub> plus CDDO-Im (Figure S1) as well as from three age-matched untreated animals. All of these samples were obtained from a model study that induced nearly complete incidence of HCC in rats and total HCC protection with CDDO-Im<sup>34</sup>. At the time the tissue samples used for the current study were collected, the animals had not been exposed to AFB<sub>1</sub> for almost one year.

RNA sequencing results yielded an average of 14,132,166 clean reads for non-tumor tissues from untreated animals, 20,674,284 clean reads for tumors induced by AFB<sub>1</sub>, and 19,568,578 clean reads for non-tumor tissues from animals co-exposed to AFB<sub>1</sub> plus CDDO-Im. The miRNA database miRBase ([www.mirbase.org](http://www.mirbase.org)) was used to explore the aligned miRNA reads, revealing a total of 598 identified miRNAs. Of the identified miRNAs, 176 miRNAs were significantly expressed, as determined by abundances over 50 reads per million aligned miRNA reads. The majority of microRNAs (71%, 125 miRNAs) shared expression in the tissues of animals from all three groups (Figure 1). Twenty-two miRNAs (12.5%) were exclusively expressed in tumors and zero miRNAs were significantly co-expressed in tumors and non-tumor tissues from the AFB<sub>1</sub> and AFB<sub>1</sub> plus CDDO-Im treatment groups, respectively. The miRNA rno-mir-339-5p was found predominantly in non-tumor tissues from the AFB<sub>1</sub> plus CDDO-Im group (Table 1). We found twelve miRNAs uniquely expressed in the hepatic tissue of untreated animals. Pairwise comparison analysis revealed 114 miRNAs differentially expressed in tumors and the age-matched livers of the intervention animals (Table S2).

**Validation of sequencing data by RT-qPCR**—To validate RNA sequencing data, a panel of miRNAs was selected for follow-up by real-time PCR analysis. Candidate miRNAs were selected by calculating ratios of miRNA count data between treatment groups, and then creating a list of top miRNAs with a dynamic range greater than a five-fold change (tumor vs. non-tumor). The following miRNAs were selected because they were most dysregulated according to these criteria: rno-miR-802-5p, 31a-5p, 224-5p, 10b-5p, 31a-5p, 205, 132-3p,

141–3p, 182, 200b–3p, and 429 (Table 2). Rno-miR-122–5p was also included because of its normal role within the liver. Of the eleven candidate miRNAs, nine were upregulated in aflatoxin-induced tumors whereas rno-miR-802–5p and 122–5p were down regulated in tumors and strongly expressed in non-tumor tissue from animals previously co-exposed to CDDO-Im.

Figure 2 represents the candidate miRNA expression results obtained from PCR validation. In tumors, the expression of rno-miR-132–3p, 141–3p, 10b–5p, 31a–5p, 429, 182, 200b–3p, 205, and 224–5p were increased compared to non-tumor tissue from CDDO-Im intervention animals. Rno-miR-224–5p had the largest significant increase (~700 fold). The expression of these candidate miRNAs was much lower in all non-tumor tissue from animals previously dosed with AFB<sub>1</sub> plus CDDO-Im, with the exception of rno-miR-802–5p, as seen in sequencing results.

### 3.2 Candidate miRNA levels in sera at the termination of the study

To examine whether the expression levels of candidate miRNAs measured in tumors and non-tumor tissues parallel levels in circulation, unfractionated sera from the same animals used for RNA sequencing were analyzed at the time of sacrifice by real-time PCR. All candidate miRNAs were detectable in sera. Figure 3 depicts that rno-miRs-182 and 122–5p were significantly increased in the circulation of animals diagnosed with HCC when compared to intervention animals. Increased circulating levels of rno-miR-224–5p, 802–5p, and 31a–5p were also observed in animals diagnosed with HCC, although the findings were not statistically significant.

### 3.3 Temporal changes in circulating miRNA levels

The samples analyzed and shown in Figure 3 were obtained at the most advanced stages of HCC (shown in AFB<sub>1</sub> dosed animals in Figure S1) when necrosis and other biological processes occurring may skew the alteration of serum miRNA levels. Since longitudinal serum samples had been collected at monthly intervals, miRNA levels in the circulation of animals across the trajectory to disease could be explored. This would allow identifying the emergence of miRNAs that may be attributable to the disease process and therefore be predictive. The sera obtained starting at 17 weeks of age and continuing monthly until sacrifice were analyzed by qPCR. It is also important to note that aflatoxin-treated animals began to develop palpable tumors around 70 weeks of age, which was observed during blood collection. For many of the candidate miRNAs, the circulating levels were similar between treatment groups with fold changes less than 2 (e.g. rno-miR-224–5p, 10b–5p, 429, 200b–3p) (Figure 4). In Figure 4 are shown miR-122–5p and miR-802–5p, and miR-182 displayed in Figure 5 revealed statistically significant differences in circulating levels between treatment groups, with fold changes of 4.66 (95% CI: 3.49–6.23), 2.60 (95% CI: 1.82–3.71), and 5.13-fold change (95% CI: 4.59–5.70), respectively. Serum rno-miR-182 was the only miRNA that tracked with a significant difference in levels between the aflatoxin and aflatoxin plus CDDO-Im dosed animals at every time point (Figure 5). This difference was further amplified when measuring rno-miR-182 levels in terminal sera (filled symbols).

## 4. Discussion

In this study, analysis of a unique sample set allowed for the identification of miRNAs dysregulated in HCC progression. This sample set was obtained from a quantitative rat cancer model where the individualized outcomes were known for each animal following their initiation of carcinogenesis during a 28-day dosing regimen<sup>34</sup>. Of the animals selected for further analysis in this study, those dosed with AFB<sub>1</sub> began to develop palpable tumors and concomitant weight loss at 70 or more weeks of age and were formally diagnosed with HCC at the time of sacrifice (Figure S1). Animals in the AFB<sub>1</sub> plus CDDO-Im group did not develop HCC (Figure S1). Transcriptomic analysis of tumors from aflatoxin-treated animals and non-tumor tissues from animals co-exposed to the chemopreventive agent CDDO-Im exhibited a perturbed global miRNA profile in tumors. Specifically, rno-miRs-224-5p, 205, 200b-3p, 182, 429, 31a-5p, 10b-5p, 141-3p, 132-3p, and 802-5p were found to be the most dysregulated. The sequences were also verified for homology to the respective human miRs. MiR-224-5p is noted in the literature to be commonly upregulated in HCC, can promote tumor cell migration and invasion, and targets cell cycle checkpoints such as, *p21*<sup>26,38</sup>. Elevated serum levels of this miR have also been observed in early stages of HCC<sup>26</sup>. Rno-miR-31a-5p is increased in plasma after liver injury and differs from its human homolog hsa-miR-31 by one nucleotide<sup>36,39,40</sup>. In humans, miR-31 is associated with aging livers and is increased in tumors, correlating with cirrhosis<sup>28,41,42</sup>. Other miRNAs found upregulated in tumors, such as the miR-200 family (e.g. rno-miRs-200b-3p, 429, 141-3p) and rno-miR-205 are known to play a role in angiogenesis and epithelial to mesenchymal transition in multiple cancers including HCC<sup>43,44</sup>. MiR-802-5p was the only candidate selected that was significantly decreased in tumors. This miRNA is noted to play a tumor suppressive role in different cancers and demonstrates moderate tumor suppressive activity against c-Myc driven hepatocarcinogenesis in mice<sup>45</sup>. In terminal sera, however, rno-miR-802-5p was elevated in animals with HCC. This result supports a study by Wolenski *et al.* that points to this miRNA as a plasma marker of liver injury<sup>39</sup>.

Levels of serum miRs-182 and 122-5p were also elevated in animals diagnosed with HCC. Longitudinal analysis of circulating miRNAs revealed rno-miR-182 as a potential predictive biomarker, which is 96% identical in sequence to its human homolog. MiR-182 is another oncomiR that is commonly upregulated in multiple cancers and predicts poor survival in patients<sup>46-50</sup>. Chen *et al.* observed that high levels of serum miR-182 in HCC patients were significantly associated with decreased survival after surgery<sup>22</sup>. Functionally, this miRNA targets tumor suppressor genes CCAAT enhancer binding protein (CEBPA) and forkhead box O 1 (FOXO1)<sup>48,51</sup>. It has been also shown to affect WNT/ $\beta$ -catenin and AKT signaling by targeting forkhead box O 3a (FOXO3a) in tumor tissue which resulted in HCC proliferation<sup>52</sup>. Within this study, increased miR-182 could be altering these signaling pathways and increasing tumor cell proliferation. While we did not investigate the origin of serum candidate miRNAs, miR-182 could be acting after release from cancer cells or from cells reprogrammed due to injury by AFB<sub>1</sub> (e.g., encapsulated in exosomes). We did not use imaging to track the development of hepatic tumors; however, they did not become palpable until about 70 weeks of age in the AFB<sub>1</sub>-treated rats. Given the detection of miR-182 in sera at 17 weeks, it is likely its elevated expression initially arises from pre-neoplastic tissue

earlier in the carcinogenic process. Significant spikes in serum miR-182 were observed between the last scheduled monthly sample to the terminal sample in 4 out of 5 tumor-bearing rats, suggesting that tumors are nonetheless a substantial source. This aspect should be investigated in future experiments. The results from the present study show significant elevation of this miRNA in sera observed less than two months after the AFB<sub>1</sub> dosing period and considerably before diagnosis (sacrifice). It is remarkable that this increase is maintained throughout the lifetimes of the animals during such a complex and multifactorial disease like cancer. To our knowledge, this is the first study to indicate a miRNA that is truly predictive for risk stratification of hepatocellular carcinoma.

In summary, the results presented here describe a panel of miRNAs highly dysregulated in aflatoxin-induced hepatic tumors. This dysregulation translates to sera for miRs-122-5p and 182, with the latter displaying increased expression throughout development of disease. Further validation of this finding is needed in human samples. For example, future experiments could measure serum miR-182 levels in random samples from a prospective human HCC study. In addition, serum miRs-122-5p and 802-5p could be explored as potential biomarkers as these also were significantly elevated throughout the lifetimes of animals with HCC. Validation of serum miR-182 can lead to alternative screening and surveillance methods for individuals with high risk of developing HCC.

## Supplementary Material

Refer to Web version on PubMed Central for supplementary material.

## Acknowledgements

We thank the Next Generation Sequencing Center (Sidney Kimmel Comprehensive Cancer Center, Johns Hopkins School of Medicine) for assistance with RNA sequencing and data analysis.

Funding Support:

This research supported by NIH grants T32 ES007141, P30 CA006973, and R35 CA197222.

## Abbreviations:

<b>AFB<sub>1</sub></b>	Aflatoxin B <sub>1</sub>
<b>CDDO-Im</b>	1-[2-cyano-3-,12-dioxooleana-1,9(11)-dien-28-oyl]imidazole
<b>miRNA or miR</b>	microRNA
<b>HCC</b>	hepatocellular carcinoma

## References

1. Naghavi M, Abajobir AA, Abbafati C, et al. Global, regional, and national age-sex specific mortality for 264 causes of death, 1980–2013;2016: a systematic analysis for the Global Burden of Disease Study 2016. *The Lancet*. 390(10100):1151–1210.
2. Llovet JM, Zucman-Rossi J, Pikarsky E, et al. Hepatocellular carcinoma. *Nat Rev Dis Primers*. 2016;2:16018. [PubMed: 27158749]



3. Mazzanti R, Arena U, Tassi R. Hepatocellular carcinoma: Where are we? *World Journal of Experimental Medicine*. 2016;6(1):21–36. [PubMed: 26929917]
4. Santi V, Trevisani F, Gramenzi A, et al. Semiannual surveillance is superior to annual surveillance for the detection of early hepatocellular carcinoma and patient survival. *J Hepatol*. 2010;53(2):291–297. [PubMed: 20483497]
5. Tsuchiya N, Sawada Y, Endo I, Saito K, Uemura Y, Nakatsura T. Biomarkers for the early diagnosis of hepatocellular carcinoma. *World journal of gastroenterology : WJG*. 2015;21(37):10573–10583. [PubMed: 26457017]
6. Torre LA, Siegel RL, Ward EM, Jemal A. Global Cancer Incidence and Mortality Rates and Trends--An Update. *Cancer Epidemiol Biomarkers Prev*. 2016;25(1):16–27. [PubMed: 26667886]
7. Shah S, Bellows BA, Adedipe AA, Totten JE, Backlund BH, Sajed D. Perceived barriers in the use of ultrasound in developing countries. *Critical Ultrasound Journal*. 2015;7:11.
8. Ahsani Z, Mohammadi-Yeganeh S, Kia V, Karimkhanloo H, Zarghami N, Paryan M. WNT1 Gene from WNT Signaling Pathway Is a Direct Target of miR-122 in Hepatocellular Carcinoma. *Applied biochemistry and biotechnology*. 2017;181(3):884–897. [PubMed: 27687586]
9. Mohamed AA, Ali-Eldin ZA, Elbedewy TA, El-Serafy M, Ali-Eldin FA, AbdelAziz H. MicroRNAs and clinical implications in hepatocellular carcinoma. *World journal of hepatology*. 2017;9(23):1001–1007. [PubMed: 28878865]
10. Li XY, Feng XZ, Tang JZ, et al. MicroRNA-200b inhibits the proliferation of hepatocellular carcinoma by targeting DNA methyltransferase 3a. *Mol Med Rep*. 2016.
11. Li Y, Di C, Li W, et al. Oncomirs miRNA-221/222 and Tumor Suppressors miRNA-199a/195 Are Crucial miRNAs in Liver Cancer: A Systematic Analysis. *Digestive Diseases and Sciences*. 2016:1–13. [PubMed: 26576552]
12. Zhuang LK, Yang YT, Ma X, et al. MicroRNA-92b promotes hepatocellular carcinoma progression by targeting Smad7 and is mediated by long non-coding RNA XIST. *Cell death & disease*. 2016;7:e2203. [PubMed: 27100897]
13. de Rie D, Abugessaisa I, Alam T, et al. An integrated expression atlas of miRNAs and their promoters in human and mouse. *Nature biotechnology*. 2017;35(9):872–878.
14. Xu J, Zhang R, Shen Y, Liu G, Lu X, Wu CI. The evolution of evolvability in microRNA target sites in vertebrates. *Genome research*. 2013;23(11):1810–1816. [PubMed: 24077390]
15. Vickers KC, Remaley AT. Lipid-based carriers of microRNAs and intercellular communication. *Current opinion in lipidology*. 2012;23(2):91–97. [PubMed: 22418571]
16. Valadi H, Ekstrom K, Bossios A, Sjostrand M, Lee JJ, Lotvall JO. Exosome-mediated transfer of mRNAs and microRNAs is a novel mechanism of genetic exchange between cells. *Nature Cell Biology*. 2007;9(6):654–U672. [PubMed: 17486113]
17. Okajima W, Komatsu S, Ichikawa D, et al. Circulating microRNA profiles in plasma: identification of miR-224 as a novel diagnostic biomarker in hepatocellular carcinoma independent of hepatic function. *Oncotarget*. 2016;7(33):53820–53836. [PubMed: 27462777]
18. Zhu Q, Gong L, Wang J, et al. miR-10b exerts oncogenic activity in human hepatocellular carcinoma cells by targeting expression of CUB and sushi multiple domains 1 (CSMD1). *BMC Cancer*. 2016;16(1):806. [PubMed: 27756250]
19. Yin J, Hou P, Wu Z, Wang T, Nie Y. Circulating miR-375 and miR-199a-3p as potential biomarkers for the diagnosis of hepatocellular carcinoma. *Tumor Biology*. 2015;36(6):4501–4507. [PubMed: 25618599]
20. Niu JX, Meng XK, Ren JJ. Studied microRNA gene expression in human hepatocellular carcinoma by microRNA microarray techniques. *World journal of gastroenterology : WJG*. 2015;21(44):12605–12611. [PubMed: 26640336]
21. Jiang L, Cheng Q, Zhang BH, Zhang MZ. Circulating microRNAs as biomarkers in hepatocellular carcinoma screening: a validation set from China. *Medicine*. 2015;94(10):e603. [PubMed: 25761179]
22. Chen L, Chu F, Cao Y, Shao J, Wang F. Serum miR-182 and miR-331–3p as diagnostic and prognostic markers in patients with hepatocellular carcinoma. *Tumour Biol*. 2015;36(10):7439–7447. [PubMed: 25903466]

23. Wang H, Hou L, Li A, Duan Y, Gao H, Song X. Expression of Serum Exosomal MicroRNA-21 in Human Hepatocellular Carcinoma. *BioMed Research International*. 2014;2014:864894. [PubMed: 24963487]
24. Liu AM, Yao TJ, Wang W, et al. Circulating miR-15b and miR-130b in serum as potential markers for detecting hepatocellular carcinoma: a retrospective cohort study. *BMJ open*. 2012;2(2):e000825.
25. Yamamoto Y, Kosaka N, Tanaka M, et al. MicroRNA-500 as a potential diagnostic marker for hepatocellular carcinoma. *Biomarkers*. 2009;14(7):529–538. [PubMed: 19863192]
26. Lin L, Lu B, Yu J, Liu W, Zhou A. Serum miR-224 as a biomarker for detection of hepatocellular carcinoma at early stage. *Clin Res Hepatol Gastroenterol*. 2016;40(4):397–404. [PubMed: 26724963]
27. Gougelet A, Sartor C, Bachelot L, et al. Antitumour activity of an inhibitor of miR-34a in liver cancer with beta-catenin-mutations. *Gut*. 2015.
28. Karakatsanis A, Papaconstantinou I, Gazouli M, Lyberopoulou A, Polymeneas G, Voros D. Expression of microRNAs, miR-21, miR-31, miR-122, miR-145, miR-146a, miR-200c, miR-221, miR-222, and miR-223 in patients with hepatocellular carcinoma or intrahepatic cholangiocarcinoma and its prognostic significance. *Mol Carcinog*. 2013;52(4):297–303. [PubMed: 22213236]
29. Liu C, Yu H, Zhang Y, et al. Upregulation of miR-34a-5p antagonizes AFB1-induced genotoxicity in F344 rat liver. *Toxicol*. 2015;106:46–56. [PubMed: 26385312]
30. Yang W, Lian J, Feng Y, et al. Genome-wide miRNA-profiling of aflatoxin B1-induced hepatic injury using deep sequencing. *Toxicology Letters*. 2014;226(2):140–149. [PubMed: 24472605]
31. Livingstone MC, Johnson NM, Roebuck BD, Kensler TW, Groopman JD. Profound changes in miRNA expression during cancer initiation by aflatoxin B1 and their abrogation by the chemopreventive triterpenoid CDDO-Im. *Mol Carcinog*. 2017;56(11):2382–2390. [PubMed: 28218475]
32. Yates MS, Tauchi M, Katsuoka F, et al. Pharmacodynamic characterization of chemopreventive triterpenoids as exceptionally potent inducers of Nrf2-regulated genes. *Mol Cancer Ther*. 2007;6(1):154–162. [PubMed: 17237276]
33. Cuadrado A, Rojo AI, Wells G, et al. Therapeutic targeting of the NRF2 and KEAP1 partnership in chronic diseases. *Nat Rev Drug Discov* 2019.
34. Johnson NM, Egnor PA, Baxter VK, et al. Complete protection against aflatoxin B(1)-induced liver cancer with a triterpenoid: DNA adduct dosimetry, molecular signature, and genotoxicity threshold. *Cancer Prev Res (Phila)*. 2014;7(7):658–665. [PubMed: 24662598]
35. Wen X, Donepudi AC, Thomas PE, Slitt AL, King RS, Aleksunes LM. Regulation of Hepatic Phase II Metabolism in Pregnant Mice. *The Journal of Pharmacology and Experimental Therapeutics*. 2013;344(1):244–252. [PubMed: 23055538]
36. Kozomara A, Griffiths-Jones S. miRBase: annotating high confidence microRNAs using deep sequencing data. *Nucleic Acids Research*. 2014;42(D1):D68–D73. [PubMed: 24275495]
37. Livak KJ, Schmittgen TD. Analysis of relative gene expression data using real-time quantitative PCR and the 2<sup>-</sup>(Delta Delta C(T)) Method. *Methods*. 2001;25(4):402–408. [PubMed: 11846609]
38. An F, Olaru AV, Mezey E, et al. MicroRNA-224 Induces G1/S Checkpoint Release in Liver Cancer. *Journal of clinical medicine*. 2015;4(9):1713–1728. [PubMed: 26343737]
39. Wolenski FS, Shah P, Sano T, et al. Identification of microRNA biomarker candidates in urine and plasma from rats with kidney or liver damage. *Journal of applied toxicology : JAT* 2017;37(3):278–286. [PubMed: 27397436]
40. Smith A, Calley J, Mathur S, et al. The Rat microRNA body atlas; Evaluation of the microRNA content of rat organs through deep sequencing and characterization of pancreas enriched miRNAs as biomarkers of pancreatic toxicity in the rat and dog. *BMC genomics*. 2016;17:694. [PubMed: 27576563]
41. Capri M, Olivieri F, Lanzarini C, et al. Identification of miR-31-5p, miR-141-3p, miR-200c-3p, and GLT1 as human liver aging markers sensitive to donor-recipient age-mismatch in transplants. *Aging cell*. 2017;16(2):262–272. [PubMed: 27995756]

42. Wojcicka A, Swierniak M, Kornasiewicz O, et al. Next generation sequencing reveals microRNA isoforms in liver cirrhosis and hepatocellular carcinoma. *The international journal of biochemistry & cell biology*. 2014;53:208–217. [PubMed: 24875649]
43. Dhayat SA, Mardin WA, Kohler G, et al. The microRNA-200 family--a potential diagnostic marker in hepatocellular carcinoma? *J Surg Oncol*. 2014;110(4):430–438. [PubMed: 24895326]
44. Gregory PA, Bert AG, Paterson EL, et al. The miR-200 family and miR-205 regulate epithelial to mesenchymal transition by targeting ZEB1 and SIP1. *Nat Cell Biol*. 2008;10(5):593–601. [PubMed: 18376396]
45. Tao J, Ji J, Li X, et al. Distinct anti-oncogenic effect of various microRNAs in different mouse models of liver cancer. *Oncotarget*. 2015;6(9):6977–6988. [PubMed: 25762642]
46. Jia L, Luo S, Ren X, et al. miR-182 and miR-135b Mediate the Tumorigenesis and Invasiveness of Colorectal Cancer Cells via Targeting ST6GALNAC2 and PI3K/AKT Pathway. *Dig Dis Sci*. 2017.
47. Visani M, de Biase D, Marucci G, et al. Expression of 19 microRNAs in glioblastoma and comparison with other brain neoplasia of grades I-III. *Molecular oncology*. 2014;8(2):417–430. [PubMed: 24412053]
48. Wang C, Ren R, Hu H, et al. MiR-182 is up-regulated and targeting Cebpa in hepatocellular carcinoma. *Chin J Cancer Res*. 2014;26(1):17–29. [PubMed: 24653623]
49. Zhang QH, Sun HM, Zheng RZ, et al. Meta-analysis of microRNA-183 family expression in human cancer studies comparing cancer tissues with noncancerous tissues. *Gene*. 2013;527(1):26–32. [PubMed: 23791657]
50. Wang F, Zhong S, Zhang H, et al. Prognostic Value of MicroRNA-182 in Cancers: A Meta-Analysis. *Disease markers*. 2015;2015:482146. [PubMed: 26063957]
51. Weidinger C, Krause K, Klagge A, Karger S, Fuhrer D. Forkhead box-O transcription factor: critical conductors of cancer's fate. *Endocrine-related cancer*. 2008;15(4):917–929. [PubMed: 18775975]
52. Cao MQ, You AB, Zhu XD, et al. miR-182–5p promotes hepatocellular carcinoma progression by repressing FOXO3a. *J Hematol Oncol*. 2018;11(1):12. [PubMed: 29361949]

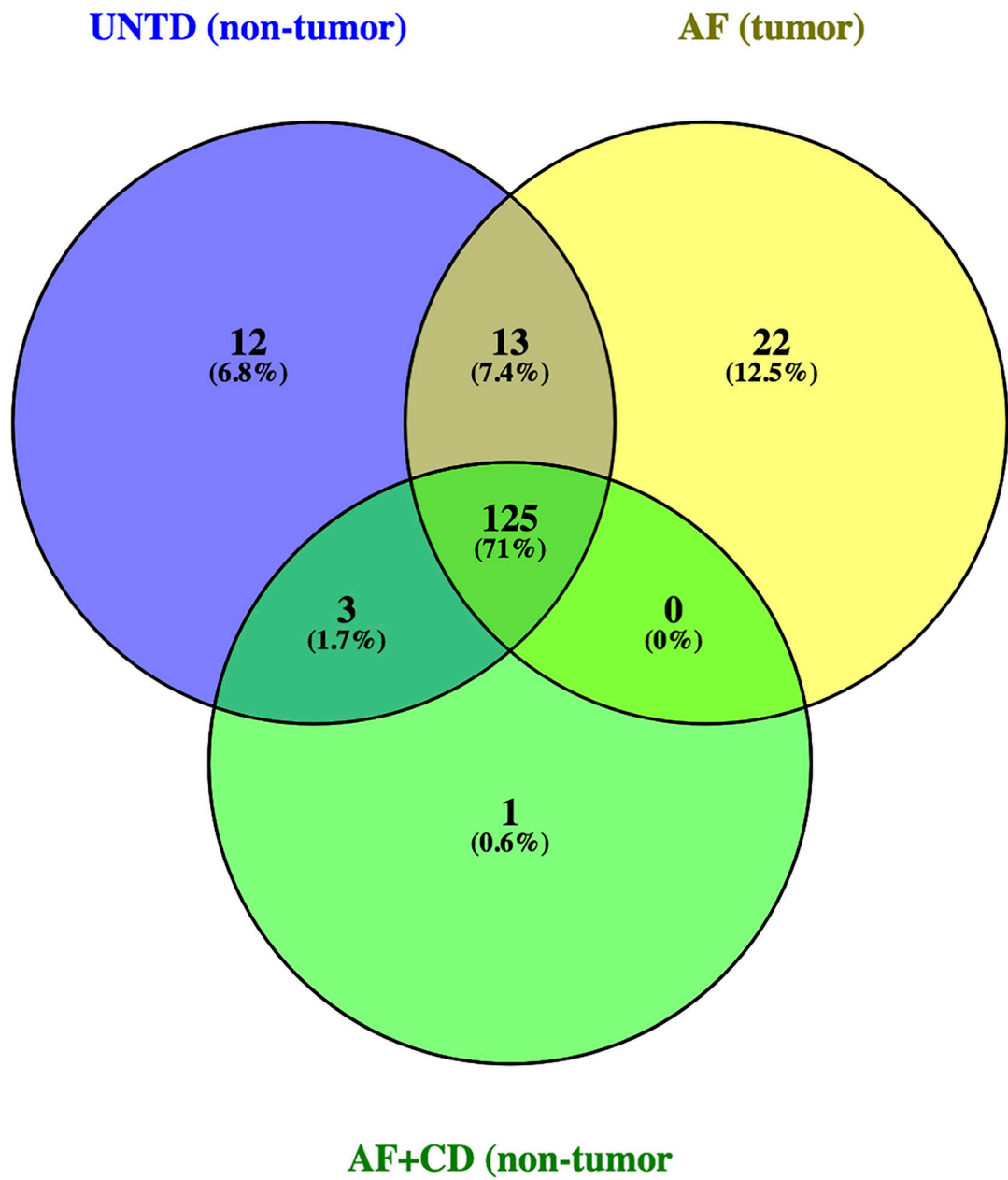


**Figure 1: Venn diagram of significantly expressed miRNAs identified by RNA-seq in untreated (UNTD; non-tumor), aflatoxin (AF; tumor), and aflatoxin plus CDDO-Im (AF+CD; non-tumor) groups.**

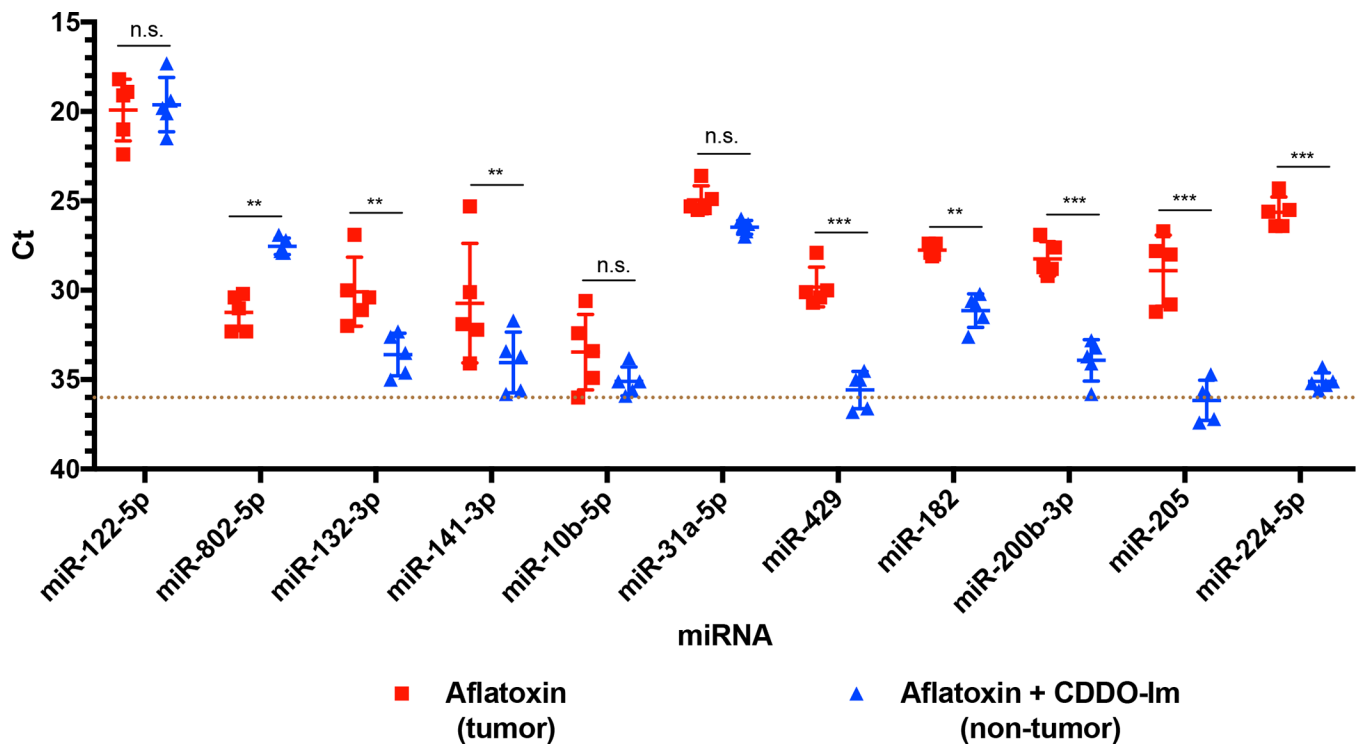


**Figure 2: Candidate miRNA expression in AFB<sub>1</sub> tumor and AFB<sub>1</sub> plus CDDO-Im non-tumor tissue.**

Real-time PCR analysis of miRNA candidates in aflatoxin-induced tumors and non-tumor tissue from CDDO-Im intervention animals (n=10). Error bars denote mean ± SD. Dotted line at y=36 indicates limit of quantitation. Difference between treatment groups: n.s., not significant; \*, p<0.05; \*\*, p<0.005, \*\*\*, p<0.001.

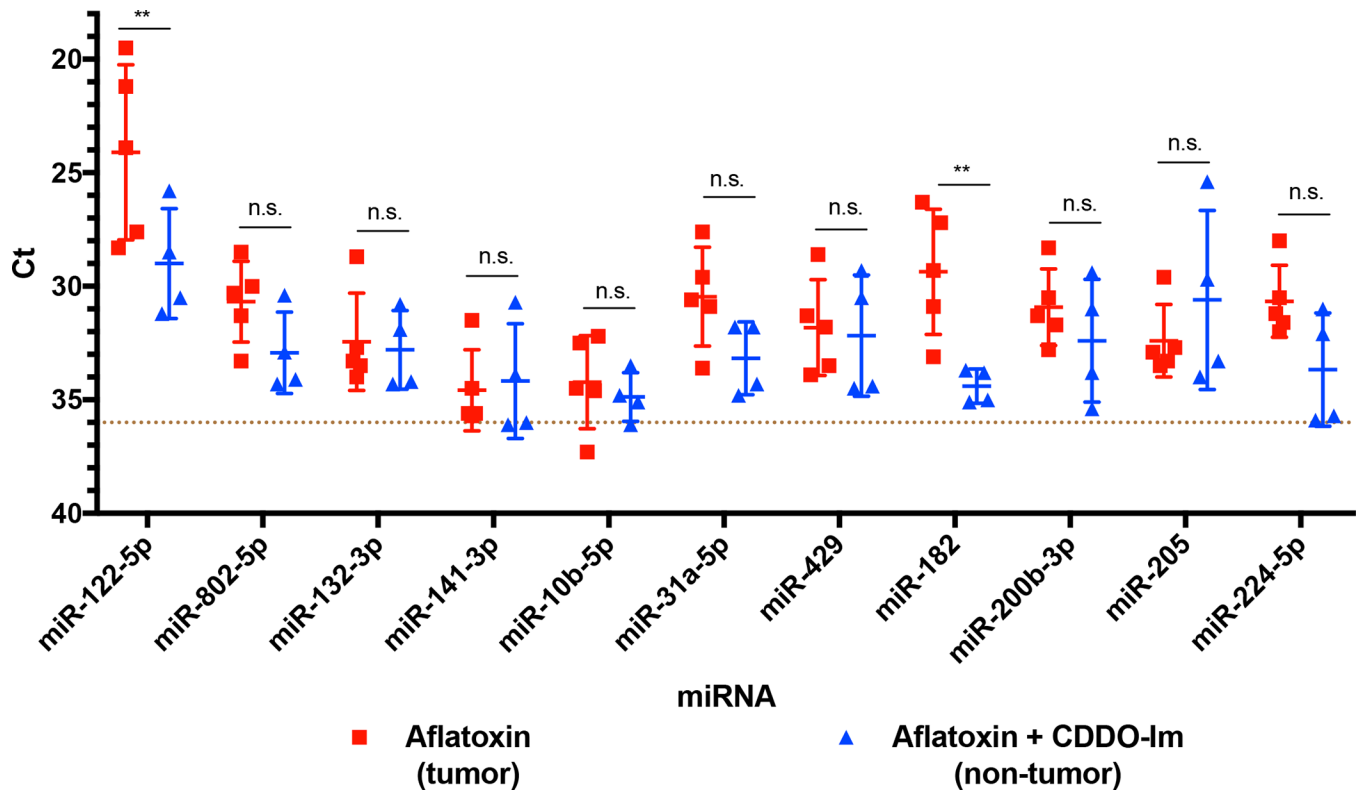


**Figure 3: Candidate miRNA expression in terminal sera.**

Real-time PCR analysis of miRNA candidates in sera from previously aflatoxin-exposed and aflatoxin plus CDDO-Im co-exposed animals (n=10). Error bars denote mean  $\pm$  SD. Dotted line at  $y=36$  indicates limit of quantitation. Difference between treatment groups: n.s., not significant; \*,  $p<0.05$ ; \*\*,  $p<0.005$ ; \*\*\*,  $p<0.001$ .

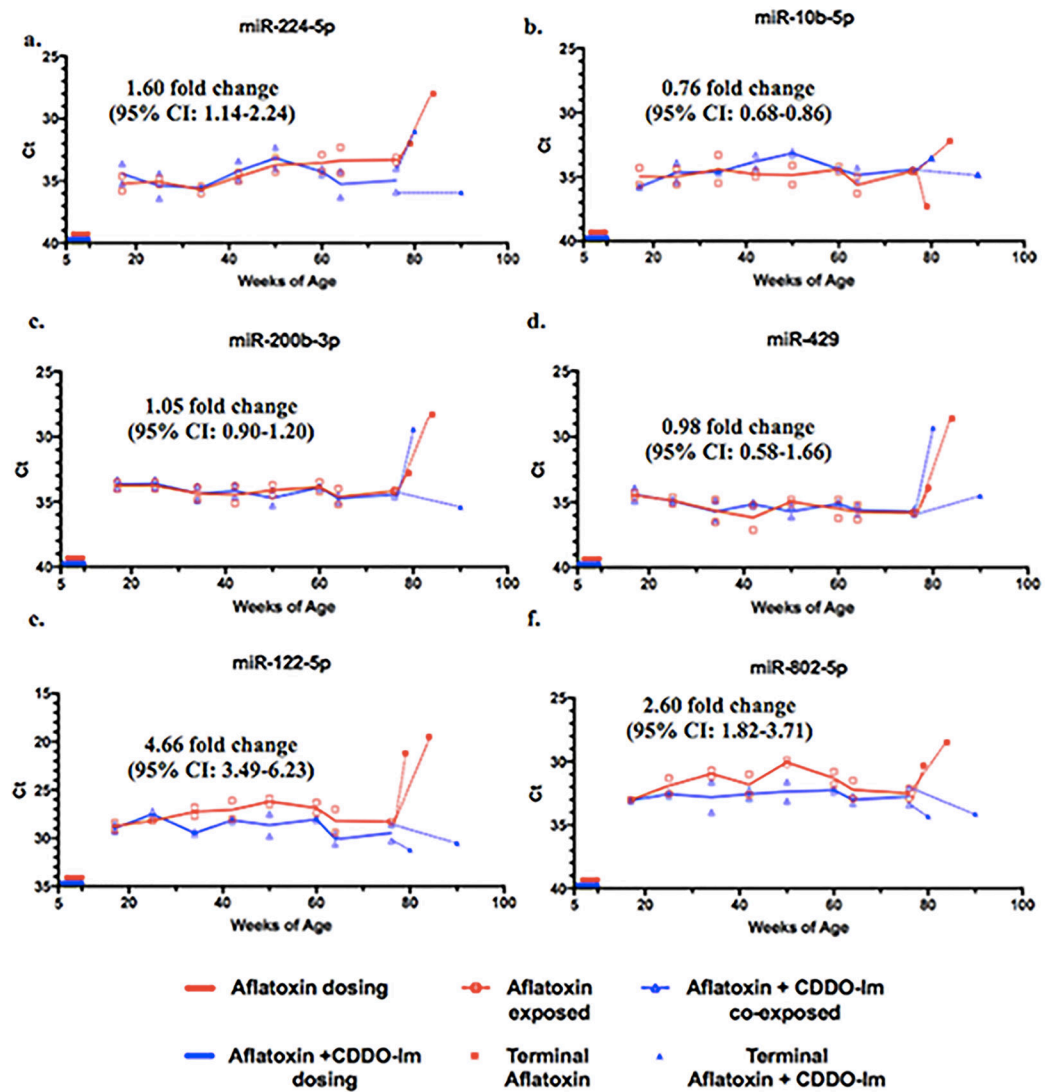


**Figure 4: Longitudinal analysis of candidate miRNAs in serum.**

Repetitive measurements of candidate miRNAs from the sera of previously aflatoxin-exposed and aflatoxin plus CDDO-Im co-exposed animals by real-time PCR (n=10). Open symbols indicate individual replicates with means connected. Closed symbols indicate miRNA levels at time of sacrifice.

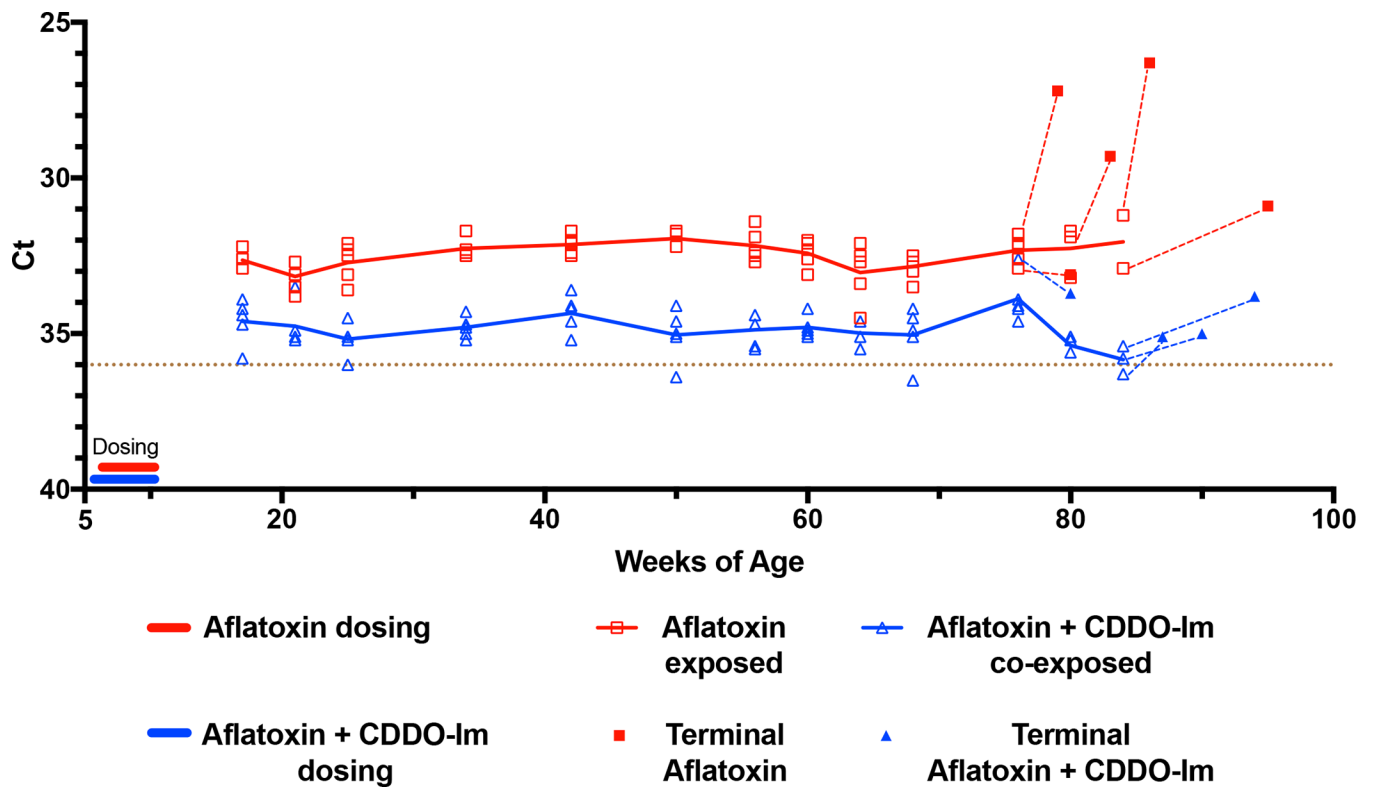


**Figure 5: Longitudinal analysis of serum miR-182.**

Repetitive measurements of serum rno-miR-182 from aflatoxin-exposed and aflatoxin plus CDDO-Im co-exposed animals by real-time PCR (n=10). Open symbols indicate individual replicates with means connected. Closed symbols indicate miRNA levels at time of sacrifice. Dotted line at  $y=36$  indicates limit of quantitation.



**Table 1:**

List of exclusive and shared miRNAs by treatment group

<b>Group</b>	<b>MicroRNAs</b>
<b>Tumors (AF) only</b>	224-5p, 205, 499-5p, 132-3p, 181d-5p, 201-5p, 221-3p, 200c-3p, 96-5p, 541-5p, 27b-5p, 598-3p, 664-3p, 155-5p, 181c-3p, 652-3p, 872-3p, 3068-3p, 195-3p, 214-3p, 361-3p, 138-5p
<b>Untreated only</b>	363-3p, 153-3p, 147, 130b-3p, 342-3p, 9a-5p, 449a-5p, 7a-5p, 139-5p, 30c-1-3p, 140-5p, 6215
<b>Untreated and Intervention (AF+CD)</b>	203b-3p, 144-3p, 144-5p
<b>Intervention (AF+CD)</b>	339-5p

Identified by RNA sequencing. Ordered by decreasing abundance.

**Table 2:**

List of candidate miRNAs and expression abundances by RNA sequencing

miRNA (rno)	Average count			Overall Ratio (UNTD:AFT:CD)	% Reduction by CDDO-Im	Ratio		
	UNTD*	AFT <sup>†</sup>	CD <sup>‡</sup>			AFT:UNTD	CD:UNTD	AFT:CD
miR-10b-5p	358	10797	290	1:30:1	97	30:1	1:1	37:1
miR-132-3p	24	119	4	1:5:0	96	5:1	0:1	27:1
miR-200b-3p	417	2294	50	1:6:0	98	6:1	0:1	46:1
miR-205	12	203	2	1:17:0	99	17:1	0:1	92:1
miR-224-5p	1	388	1	1:555:1	100	555:1	1:1	388:1
miR-429	220	1074	40	1:5:0	96	5:1	0:1	27:1
miR-31a-5p	906	4993	1087	1:6:1	78	6:1	1:1	5:1
miR-141-3p	328	1800	95	1:6:0	95	6:1	0:1	19:1
miR-182	2484	19864	2933	1:8:1	85	8:1	1:1	7:1
miR-802-5p	895	172	1352	1:0:2	-687	0:1	2:1	0:1
miR-122-5p	131323	58951	193087	1:1:2	-286	1:1	2:1	0:1

Identified by RNA sequencing. Normalized to aligned reads per million. Percentage change by CDDO-Im compared to aflatoxin-exposed sample (AFT).

\* UNTD, untreated (non-tumor);

<sup>†</sup> AFT, aflatoxin (tumor);<sup>‡</sup> CD, aflatoxin plus CDDO-Im (non-tumor).